reaches the upper limit of pyrolysis range, T_v. After that, the pyrolysis front continuously advances toward the centre of the particle, since the thermal wave follows the wet-dry interface. Thus, the drying and pyrolysis of a biomass particle can be considered as a coupled process with heat transfer as the controlling mechanism (Agarwal and La Nauze, 1989).

The model can be solved analytically under a pseudo-steady state simplification. A pseudo-steady state approximation means that time of thermal conduction through the dry shell of a thickness δ, $t_c \propto \rho_d c_p \delta^2 / k_d$ is small compared to the characteristies receding time of the wet-dry interface of a radius r_{wc}, $t_{wc} \propto q\rho_{wc} W_o r_{wc}^2 / k_d (T_b - T_{wc})$, and the distribution of temperature over the thickness of the dry shell is that of steady state condition.

3.2.1. Model assumptions

1. Fuel particles are isotropic and homogeneous and have constant size.
2. All moisture content is free water.
3. The drying occurs at the receding surface of the wet core, since the rate of the process is heat transfer controlled.
4. An abrupt pyrolysis occurs when the dry shell locally reaches a characteristic pyrolysis temperature, T_v. The latter is corresponding to the higher limit of the temperature range of devolatilization of biomass.
5. The temperature distributions in the outer char shell and in the intermediate dry layer are those of a steady state condition.
6. The temperature of the wet-dry interface, T_{wc}, remains constant at the saturation temperature. For simplicity, the initial temperature of the particle is equal to T_{wc}.
7. The water vapor and pyrolysis gases do not affect the heat transfer because of the existence of cracks, and no mass transfer effect is considered for the same reason.

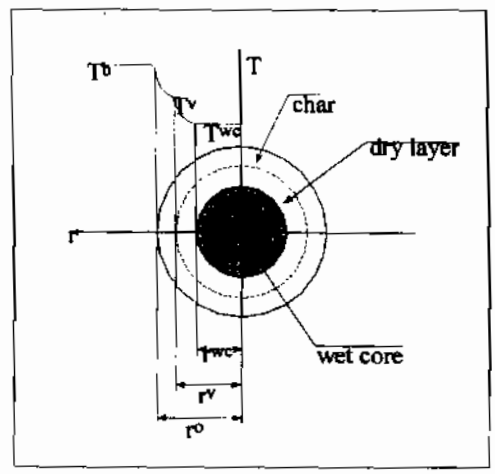

Figure 2. Different zones inside a biofuel particle during drying and devolatilization.

3.2.2. Mathematically

The energy balance for a spherical fuel particle is given by:

$$\frac{1}{r^2}\frac{\partial}{\partial}\left[r^2\frac{\partial T}{\partial r}\right]=\frac{1}{\alpha}\frac{\partial T}{\partial t} \tag{9}$$

For a pseudo state approximation the equation is reduced to

$$\frac{1}{r^2}\frac{\partial}{\partial}\left[r^2\frac{\partial T}{\partial r}\right]=0 \tag{10}$$

The equation may be put in dimentionless form

$$\frac{1}{R^2}\frac{\partial}{\partial}\left[R^2\frac{\partial \theta}{\partial R}\right]=0 \tag{11}$$

where $R=\frac{r}{r_o}$ r_o is the initial diameter of biomass particle

$\theta=\theta_c=(T-T_v)/(T_b-T_v)$ $r_o<r<r_v$

$\theta=\theta_d=(T-T_{wc})/(T_b-T_{wc})$ $r_v<r<r_{wc}$

Initial condition

$$\theta|_{\tau=0}=\theta_{wc} \tag{12}$$

Boundary conditions

-at the surface of the particle

$$\left.\frac{d\theta}{dR}\right|_{R=1}=Bi(1-\theta_s) \tag{13}$$

This condition holds for dry biomass until the surface temperature reaches T_v, $t<t_{vd}$, and for char after this instant, $t_{vd}<t<t_{vf}$;

- at the wet-dry interface

$$\theta_d|_{R_{wc}}=0 \tag{14}$$

$$\left.\frac{d\theta_d}{dR}\right|_{R_{wc}}=-\frac{dR_{wc}}{d\tau} \tag{15}$$

- at the char-dry biomass interface

$$Z\left.\frac{d\theta_c}{dR}\right|_{R_v}=\left.\frac{d\theta_d}{dR}\right|_{R_v} \tag{16}$$

where $Z=k_c(T_b-T_v)/k_d(T_b-T_{wc})$

Analytical solution of the model can be obtained provided that all thermal properties in the equations are constant with time. After many mathematical manipulations, the following expressions can be derived

Temperature distribution before starting of pyrolysis

$$\theta=\frac{R-R_{wc}}{R(1-B_dR_{wc})} \tag{17}$$

Wet core radius at beginning of devolatilization at surface of the particle

$$R_{wc,o}=\frac{1-\theta_v}{1-B_d\theta_v} \tag{18}$$

Delay period before starting of devolatilization (first period of drying)

$$\tau_1=\tau_{vd}=\frac{1}{2}\left(1-R_{wc,o}^2\right)-\frac{B_d}{3}\left(1-R_{wc\,o}^3\right) \tag{19}$$

Temperature distribution through char layer

$$\theta_c = \frac{R - R_v}{R(1 - B_c R_v)} \quad (20)$$

Temperature distribution through dry layer

$$\theta_d = \frac{(\theta_v + Z)(R - R_{wc})}{R(1 - R_{wc} B_c)} \quad (21)$$

devolatilized radius

$$R_v = \frac{R_{wc}(\theta_v + Z)}{Z + \theta_v R_{wc} B_c} \quad (22)$$

Time required for shrinking wet core, R_{wc}, after beginning of devolatilization

$$\tau = \frac{1}{\theta_v + Z}\left[\frac{1}{2}\left(R_{wc,o}^2 - R_{wc}^2\right) - \frac{B_c}{3}\left(R_{wc,o}^3 - R_{wc}^3\right)\right] \quad (23)$$

where $\tau = t/t_o$ and $t_o = q\rho_o W_o r_o^2 / k_d (T_b - T_{wc})$

Time required for complete drying of the particle after beginning of devolatilization (the second period of drying)

$$\tau_2 = \tau_{vf} = R_{wc,o}^2 (3 - 2B_c R_{wc,o}) / 6(\theta_v + Z) \quad (24)$$

Total time of particle drying

$$\tau_d = \tau_1 + \tau_2 \quad (25)$$

3.3. Char Combustion

Usually the biomass fuel particles are larger than 1 mm. So the chemical reaction of the fixed carbon is assumed to result in carbon dioxide. This assumption is in accordance with the results found by Ross and Davidson (1981).

$$C + O_2 \rightarrow CO_2 \quad (26)$$

The mass balance for a spherical particle burning following shrinking sphere model has the form

$$\frac{d}{dt}\left(\frac{\pi d_p^3}{6}\rho_{po} C_f\right) = -\mu k_{ov} C_{O2} \pi d_p^2 \quad (27)$$

The overall reaction rate coefficient k_{ov} can be expressed through the diffusion and kinetic resistance

$$\frac{1}{k_{ov}} = \frac{1}{h_m} + \frac{1}{k_c} \quad (28)$$

Assuming that μ and C_{O2} remain unchanged in the combustion process and integrating Eq. (28) between t=0 and char burn-out time t_c, the following expression estimate the average overall reaction rate coefficient,

$$k_{ov} = \frac{1}{2}\frac{\rho_{po} C_{fc} d_{po}}{\mu t_c C_{O2}} \quad (29)$$

One can estimate the chemical reaction rate constant k_c from the expression (28).

The temperature of burning particle can be estimated by the following expression, see Leckner et al. (1992)

$$T_p / T_b = 0.84 Ar_i^{0.05} \quad (30)$$

4. RESULTS AND DISCUSSION

The delay period of volatiles ignition time, t_{vd}, the flaming period of volatiles or volatiles release duration, t_{vf}, and the particle-char burnout time, t_c, have been visually observed and recorded. The state of a burning particle could be easily traced. During devolatilization it was mostly floating on the surface of the bed because of an intensive outflow of vapour and gas. The particle kept its shape and decreased insignificantly in size during this stage. The devolatilized and ignited char residues looked bright light on the darker background of the bed and were gradually decreasing in size. The char particles circulated within the bed, periodically rising to the surface. Some fines, probably ashes, were split off the char particle. Finally the particle crumbled into a number of sparkles and got lost out of view. At that moment the burnout time was registered.

Progress of drying and devolatilization throughout the particle layers are studied. The volume of dried layers, $V_d(t)$ and that of devolatilized layers, $V_v(t)$ are calculated as a function of time along the drying period. The ratio of $V_v(t)$ to $V_d(t)$ is used to express the lag between devolatilization and drying processes. Figure 3 represents the ratio as a function of time at various Biot numbers. It is noted that the lag between the beginning of devolatilization and beginning of drying decreases as the Biot number increases. For typical conditions, Bi=10 to 50, the lag is practically absent. The effect of the Biot number becomes insignificant at Bi>50. At the end of the drying period, the ratio is close to 1 for Biot number greater than 2. Thus the end of devolatilization of the particle coincides with the end of drying under typical conditions of FBC.

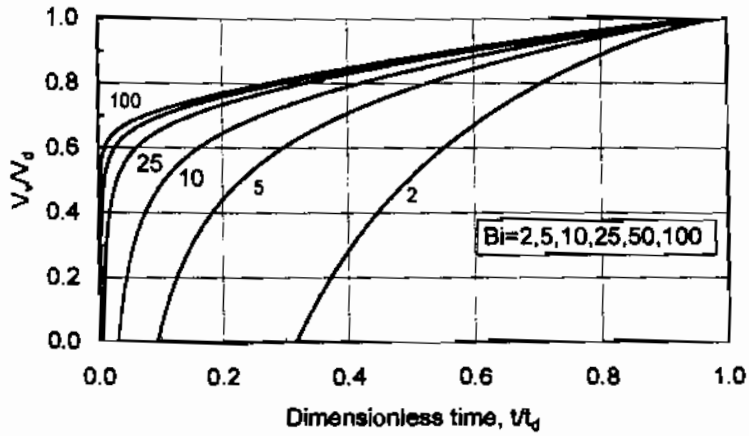

Figure 3. Ratio between volume of devolatilized layers to that of dried Layers as a function of time, at various Biot numbers.

A typical mass loss history of spherical particles of Bagasse is shown in Fig. 4. There is a good agreement between the experimental data and the calculated results.

A comparison between model results and experimental devolatilization time is presented versus the initial particle diameter in Fig. 5, for the three biofuels. Effect of moisture content is obvious. The biofuel with higher moisture content requires longer release volatile period. Bagasse has higher moisture content and requires longer volatile release period compared to robinia. On the other hand bagasse has shorter release volatile period than that of manure although bagasse has higher moisture

content. This later should be ascribed to the ash eontent of manure (17%) compare to bagasse (2%). Existence of high ash content makes the char less porous with smaller pore diameter. Thus the radiative thermal conductivity decreases. Consequently, The heat transfer rate through the particle layers is reduced making the release period of volatile longer.

The volatiles release-time can be described by empirical power-law correlations, normally used in the literature

$$t_v = k_v d_p^n \qquad (31)$$

with the parameters, k_v and n, shown in Table 2. The correlation (31) can be applied to conditions similar to those studied in the present paper.

	Bagasse	Manure	Robinia
k_v	0.577	0.624	0.42
n	1.85	1.87	1.84

Table 2. Experimental kinetic parameters of devolatilization

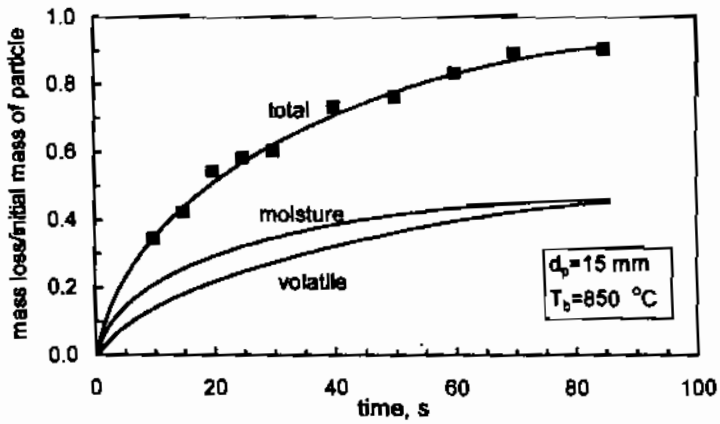

Figure 4. Mass loss histories of bagasse particle

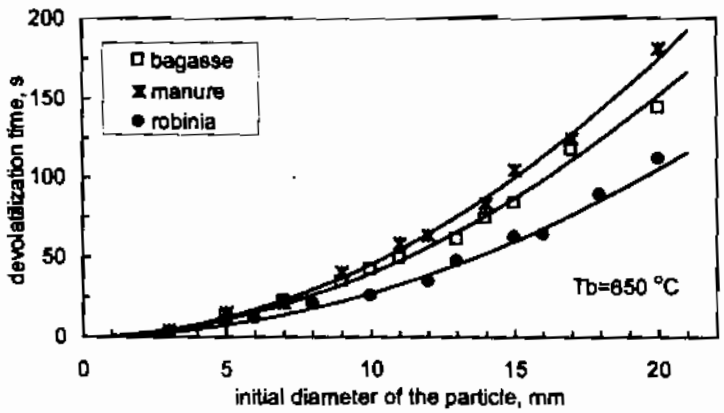

Figure 5. Comparison between experimental (symbols) and calculated (lines) volatiles release times.

The effect of bed temperature on volatile release time is shown in Fig. 6. As expected increasing bed temperature reduces the volatile release period due to increase of heat transfer rate especially by radiation.

Figure 7 represents the influence of moisture content on the volatile release period. These results could be useful for designer to choose the suitable moisture content that gives optimum combustor performance when pre-drying of biofuel is necessary.

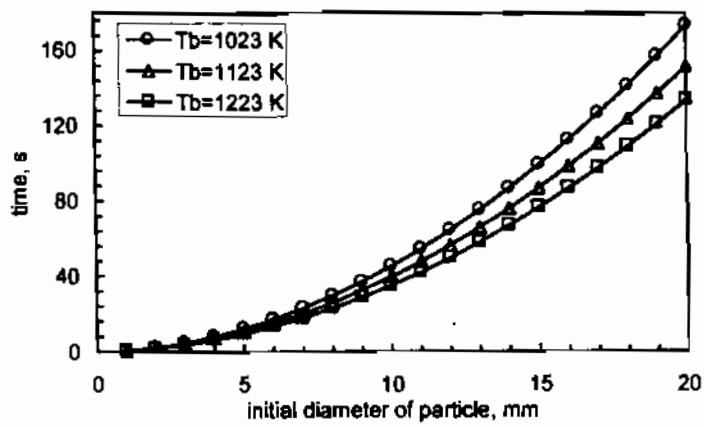

Figure 6. Influence of temperature on volatile release time.

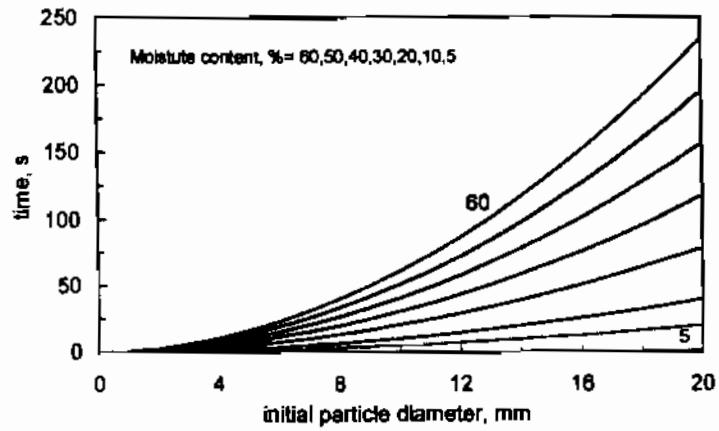

Figure 7. Effect of moisture content on volatile release time.

The Experimental overall reaction rate constant, k_{ov} evaluated by Eq. 29 is shown in Figure 8. In this figure time-average values of external mass transfer coefficients of burning particles are plotted for comparison. The time average value is obtained by integration of Eq. 1. The average chemical reaction rate constant, k_c, is estimated by Eq. (28) with k_{ov} and h_m known. At bed temperature of 850 °C the average value of k_c is found to be around 0.5, 0.2, 0.65 m/s for bagasse, manure and robinia, respectively. The low value of k_c for manure may be ascribed to its high ash content.

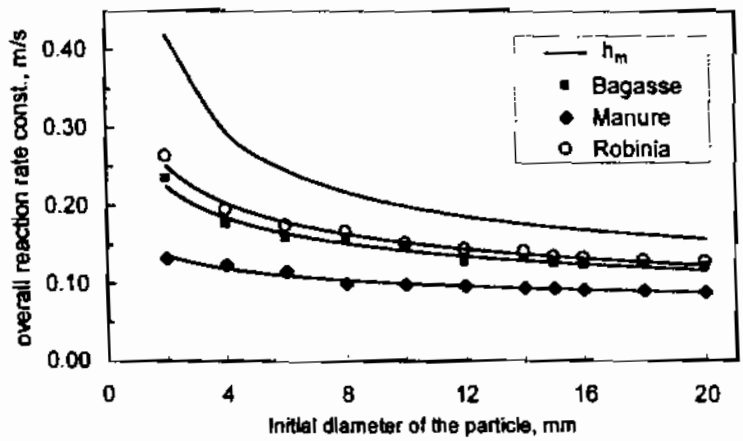

Figure 8. Experimental overall reaction rate constant at T_b=1123 K.

Figure 9 shows the char burning time as a function of initial particle diameter for the three fuels. The char burning time is estimated by Eq. 28 using k_c obtained from the experimental data. According to Eq. 28 char burning time directly increases with particle diameter. In addition, overall reaction rate constant, k_{ov} is dependent on particle diameter. k_{ov} significantly reduces with particle diameter at small diameter range and reduces slightly at large diameter, see Fig. 8. The later reason results in a more increment in time burning of char especially at small diameter. In Fig. 9 it is also noted that the burning time of char is close for the three biofuels. The explanation of this result is that the char of fuel type with higher overall reaction rate constant has higher fixed carbon content, see table 1 and Fig. 8.

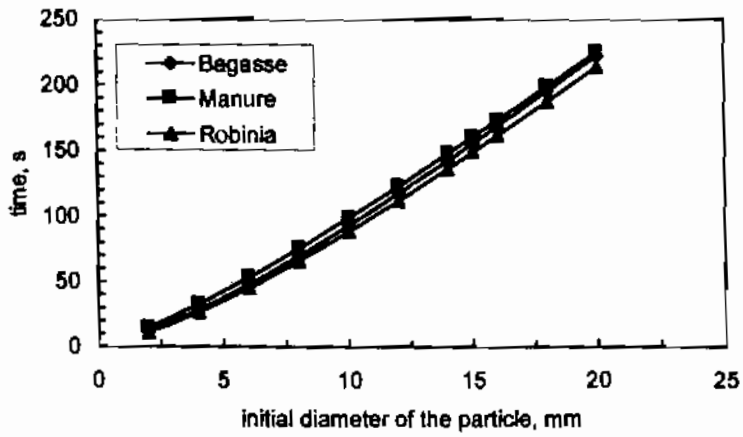

Figure 9. Char burning time as a function of initial particle diameter.

Figure 10 represents experimental values of k_c in Arrhenius' coordinates, with the data being described by the global-kinetic expression,

$$k_c = A \exp(-E/RT) \qquad (32)$$

The obtained values of the activation energy, E and constant A are (48620 kJ/kmole, 35 m/s) (65140 kJ/kmole, 68 m/s) and (41528 kJ/kmole, 27 m/s) for bagasse, manure and robinia, respectively.

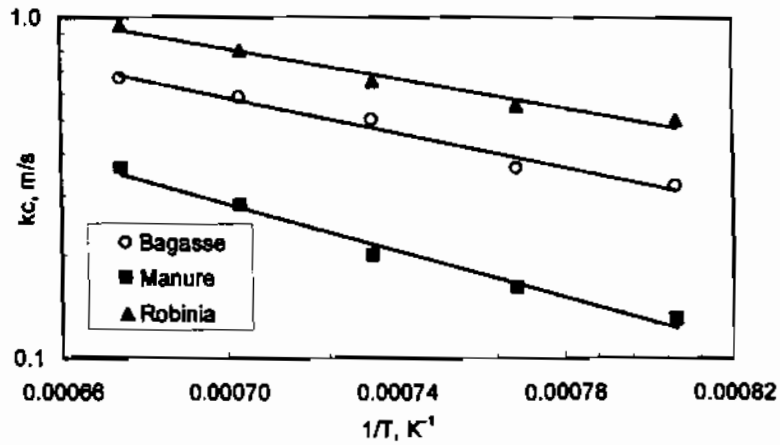

Figure 10 Arrhenius' representation of experimental data on char combustion

It can be shown for steady state combustion of mono-sized fuel that t_v/t_c is equal to the ratio of the number of devolatilized fuel particles to the number of char residues in the furnace. Experimental values of t_v/t_c are shown in Fig. 11. It is noted that t_v/t_c increases with the size of the fuel particles. Data shown in Fig. 11 are obtained at maximum oxygen concentration in the air, 21%. According to Eq. (29), the lower oxygen concentration the higher char burnout time, whereas volatiles release time practically does not change. Thus with lower oxygen concentration t_v/t_c should be reduces.

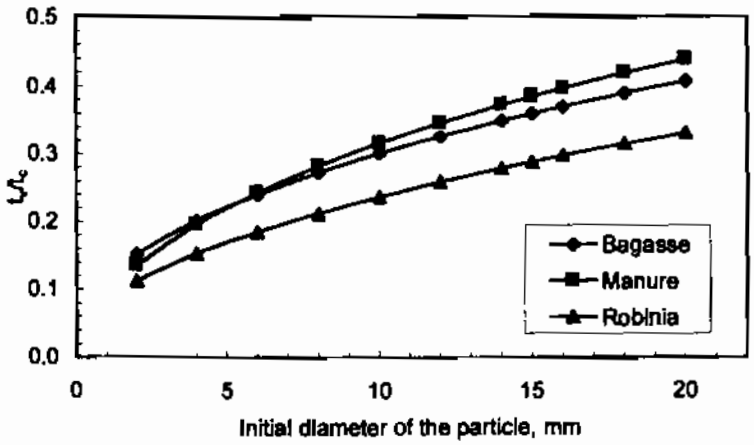

Figure 11. Ratio of volatile time to time of char combustion, at T_b=1123 K.

Table 3 compares the particle burnout times in a fluidized bed measured at an oxygen concentration of C_{02}=21 %, with predictions. There is a good agreement between predictions and experiments. The deviation is usually less than 5%.